Journal of Hydrology 552 (2017) 351–365

Contents lists available at ScienceDirect

Journal of Hydrology

journal homepage: www.elsevier.com/locate/jhydrol

Research papers

Calculating e-flow using UAV and ground monitoring

C.S. Zhao [a,b,c], C.B. Zhang [b], S.T. Yang [a,b,c,*], C.M. Liu [a], H. Xiang [d], Y. Sun [e], Z.Y. Yang [d], Y. Zhang [b], X.Y. Yu [b], N.F. Shao [b], Q. Yu [f]

[a] College of Water Sciences, Beijing Normal University, Beijing 100875, PR China
[b] Beijing Key Laboratory for Remote Sensing of Environment and Digital Cities, School of Geography, Beijing Normal University, Beijing 100875, PR China
[c] Beijing Key Laboratory of Urban Hydrological Cycle and Sponge City Technology, Beijing 100875, PR China
[d] Jinan Survey Bureau of Hydrology and Water Resources, Jinan 250013, PR China
[e] Dongying Bureau of Hydrology and Water Resources, Dongying 257000, PR China
[f] School of the Environment, Faculty of Science, University of Technology, Sydney NSW 2007, Australia

ARTICLE INFO

Article history:
Received 22 March 2017
Received in revised form 15 June 2017
Accepted 26 June 2017
Available online 8 July 2017
This manuscript was handled by Geoff Syme, Editor-in-Chief, with the assistance of Giorgio Mannina, Associate Editor

Keywords:
Environmental flows (e-flows)
Unmanned aerial vehicle (UAV)
Ground-monitored fish community

ABSTRACT

Intense human activity has led to serious degradation of basin water ecosystems and severe reduction in the river flow available for aquatic biota. As an important water ecosystem index, environmental flows (e-flows) are crucial for maintaining sustainability. However, most e-flow measurement methods involve long cycles, low efficiency, and transdisciplinary expertise. This makes it impossible to rapidly assess river e-flows at basin or larger scales. This study presents a new method to rapidly assessing e-flows coupling UAV and ground monitorings. UAV was firstly used to calculate river-course cross-sections with high-resolution stereoscopic images. A dominance index was then used to identify key fish species. Afterwards a habitat suitability index, along with biodiversity and integrity indices, was used to determine an appropriate flow velocity with full consideration of the fish spawning period. The cross-sections and flow velocity values were then combined into AEHRA, an e-flow assessment method for studying e-flows and supplying-rate. To verify the results from this new method, the widely used Tennant method was employed. The root-mean-square errors of river cross-sections determined by UAV are less than 0.25 m, which constitutes 3–5% water-depth of the river cross-sections. In the study area of Jinan city, the ecological flow velocity (V_E) is equal to or greater than 0.11 m/s, and the ecological water depth (H_E) is greater than 0.8 m. The river ecosystem is healthy with the minimum e-flow requirements being always met when it is close to large rivers, which is beneficial for the sustainable development of the water ecosystem. In the south river channel of Jinan, the upstream flow mostly meets the minimum e-flow requirements, and the downstream flow always meets the minimum e-flow requirements. The north of Jinan consists predominantly of artificial river channels used for irrigation. Rainfall rarely meets the minimum e-flow and irrigation water requirements. We suggest that the water shortage problem can be partly solved by diversion of the Yellow River. These results can provide useful information for ecological operations and restoration. The method used in this study for calculating e-flow based on a combination of UAV and ground monitoring can effectively promote research progress into basin e-flow, and provide an important reference for e-flow monitoring around the world.

1. Introduction

Today, the global increase in human activities has led to serious water pollution, water resource shortages, and uncontrolled mining and use of groundwater, resulting in river blanking, river drying, water and soil loss, water environment deterioration, and biodiversity loss (Tazioli, 2009; Joniak and Kuczyńska-Kippen, 2010; Tazioli et al., 2012; Wilbers et al., 2014; Aquilanti et al., 2016). Also groundwater scarcity and water loss can be serious environmental problems in a watershed, especially in some areas

Abbreviations: BDK, Bingdukou; BDSH, Beidashahe; DSM, digital surface model; e-flow, environmental flow; H_E, ecological water depth; HSI, habitat suitability index; HTQ, Huangtaiqiao; IBI, index of biotic integrity; JYH, Juyehe; LK, Luokou; MHSI, multispecies-based HSI; NYZ, NieYingZha; Q_E_min, minimum e-flow; RMSE, root mean square error; V_E, ecological flow velocity; UAV, Unmanned aerial vehicle; ZGNL, Zhanggongnanlin.

* Corresponding author at: Beijing Normal University, Beijing 100875, PR China.
E-mail address: yangshengtian@bnu.edu.cn (S.T. Yang).

http://dx.doi.org/10.1016/j.jhydrol.2017.06.047
0022-1694/© 2017 Elsevier B.V. All rights reserved.

of the world (Comodi et al., 2011; Tazioli et al., 2015). The river ecosystem is an important link between sediment transport and energy conversion, and is vital for maintaining a healthy basin ecosystem. However, the deterioration of basin water ecosystems and uncontrolled use of water resources cause river flows that are far below that required by the aquatic biota. This seriously affects the health of the river ecosystem. Environmental flow (E-flow) is an important index for evaluating whether water resources are reasonably exploited and utilized, and critical for maintaining a balanced ecosystem (Yang et al., 2013). Therefore, to maintain sustainable water resource use and healthy river ecosystems, it is important to further conduct valid e-flow research.

There are many methods for calculating e-flow. They can be divided into outer river and inner river methods according to ecosystem location (Cui and Zhang, 2010). The outer river mainly consists of wetlands, groundwater, vegetation, and city environments (Xu et al., 2005; Chen et al., 2012; Napiórkowska-Krzebietke and Dunalska ,2015); e-flow is indirectly calculated based on evapotranspiration, biomass, and remote sensing. In all e-flow methods, the proportion for inner river is far more than that for the outer river.

Inner river e-flow methods mainly include rivers, lakes, and estuaries, and can be roughly divided into hydrology (Armentrout and Wilson, 1987; Li et al., 2011, 2012), hydraulics (Wang et al., 2009; Peng et al., 2012; Yu et al., 2016), habitat (Stalnaker et al., 1995; Scharbert and Borcherding, 2013; Wu et al., 2014; Yang et al., 2008; Pan et al., 2015; Mackie et al., 2013), comprehensive (Shokoohi and Hong, 2011; Wang et al., 2013b; Gopal, 2016), and other methods (Chen et al., 2011; Li, 2012; Shang et al., 2014). These methods have various data requirements and can be applied to rivers with different datasets, details please refer to Liu et al. (2011) and Tharme (2003). However, with most methods, it is difficult to acquire channel parameters, and obtaining accurate data is not time- and cost-effective, necessitating transdisciplinary expertise.

Rapid assessment of river e-flows is necessary to protect or restore aquatic ecosystems, ensure sustainable use of limited water resources under intensive human activities at basin or larger scales, and maintain sufficient river flows for biota. In recent years, due to the rapid development of UAV, it has become possible to rapidly, flexibly, conveniently, and efficiently acquire ground information. These advances in UAV can effectively increase the cost-effectiveness of data collection. Therefore, a combination of UAV and ground monitoring data can promote the necessary advances in e-flow assessment.

The objective of this study is to present a new method for rapid e-flow assessment based on UAV and ground monitoring data. River-course cross-sections are critical parameters for both river flow calculation and e-flow assessment. They are retrieved using high-resolution UAV stereoscopic images, and combined into AEHRA, an e-flow assessment method by Liu et al. (2011) for studying e-flows and supplying-rate. The method in this study can rapidly assess river e-flows and help to promote the understanding and assessment of regional river health.

2. Study area and data

2.1. Study area

Jinan City, the "City of Springs" (36.0–37.5 N, 116.2–117.7E), is a pilot city for the construction of a civilized and ecological city in China. Bordered by Mount Tai to the south and traversed by the Yellow River, it has steeper topography in the south than in the north (Fig. 1). Hilly areas, piedmont clinoplain, and alluvial plains span the city from south to north. The altitude ranges from −30 to 957 m above sea level, with steep relief. The semi-humid continental monsoon climate in the city is characterized by cold, dry winters and hot, wet summers. The average annual precipitation is 636 mm, 75% of which falls during high-flow periods. The average annual temperature is 14.3 °C. The average monthly temperature is highest in July, ranging from 26.8 to 27.4 °C, and lowest in January, ranging from 1.4 to 3.2 °C (Cui et al., 2009; Zhang et al., 2010). The city represents a typical developing city in China, with an area of 8227 km^2 and a population of 5.69 million (Zhang et al., 2007). With rapid industrial development and urbanization in recent decades, the water resources in Jinan have become severely polluted and reduced through extraction (Hong et al., 2010; Zhao et al., 2015a). The pollutants mainly include high concentration of chemical oxygen demand, total nitrogen, total phosphorus and ammonia nitrogen. Policy-makers and stakeholders are aware of the need to rehabilitate the aquatic ecosystems in Jinan City. To ensure successful aquatic ecosystem restoration over all river sections at the basin scale, river administrators urgently require a method for rapid and timely estimation of e-flows to maintain sufficient river flows for aquatic ecosystems.

2.2. Data

To facilitate research programs into the rehabilitation of aquatic ecosystems in Jinan City, 59 routine monitoring stations were established, distributed evenly along main rivers (Fig. 1). At these monitoring stations, both hydrologic parameters and fish communities were concurrently measured during eight field campaigns from 2014 to 2016.

Of the 59 monitoring stations, we selected 6 typical points to assess e-flows and one to validate the method presented in this study. Among them, Bingdukou (BDK) is located on the southernmost mountain of the study area, and effectively represents the e-flow of south Jinan. Beidashahe (BDSH) is the entrance where the Yellow River flows into the study area, reflecting the Yellow River e-flow in Jinan. Luokou (LK), Huangtaiqiao (HTQ), and Juyehe (JYH) are located in the city center, representing e-flow under intense human activities. Zhanggongnanlin (ZGNL) reflects e-flow in the northern plain area. NieYingZha (NYZ) has abundant historical hydrologic data; therefore, it is used to verify the reliability of the method.

At the routine monitoring stations, hydrological parameters including water depth and flow velocity, as well as fish data, were routinely monitored. Flow velocity data were acquired by combining an electric wave current-meter (Stalker II SVR V1.0) and a traditional current meter (No. LS25-1), thereby guaranteeing the precision of the measured results. Both water depth and river width were measured using tape. River flow was calculated using flow velocity and water depth.

Fish were collected during a 30-min period in three habitat types (i.e., pools, riffles, and runs) within a 500-m section along the river at each sampling site. Fish caught from the three habitats were combined to represent each site. In wadeable streams, fish collection was performed by a two-person team (Barbour et al., 1999). In unwadeable streams, seine nets (mesh sizes of 30 and 40 mm) were used to collect fish from a boat. In addition, electrofishing was conducted to ensure that a good representation of fish species was collected at each site. All fish collected were identified in situ by species according to Chen et al. (1987) and then counted, weighed, and recorded in field data sheets. Afterwards, all identified fish were released. A few specimens that could not be identified in the field were preserved in 10% formalin solution and stored in labeled jars for subsequent laboratory identification. Table 1 shows the fish species recorded in Jinan City during the eight field campaigns from 2014 to 2016.

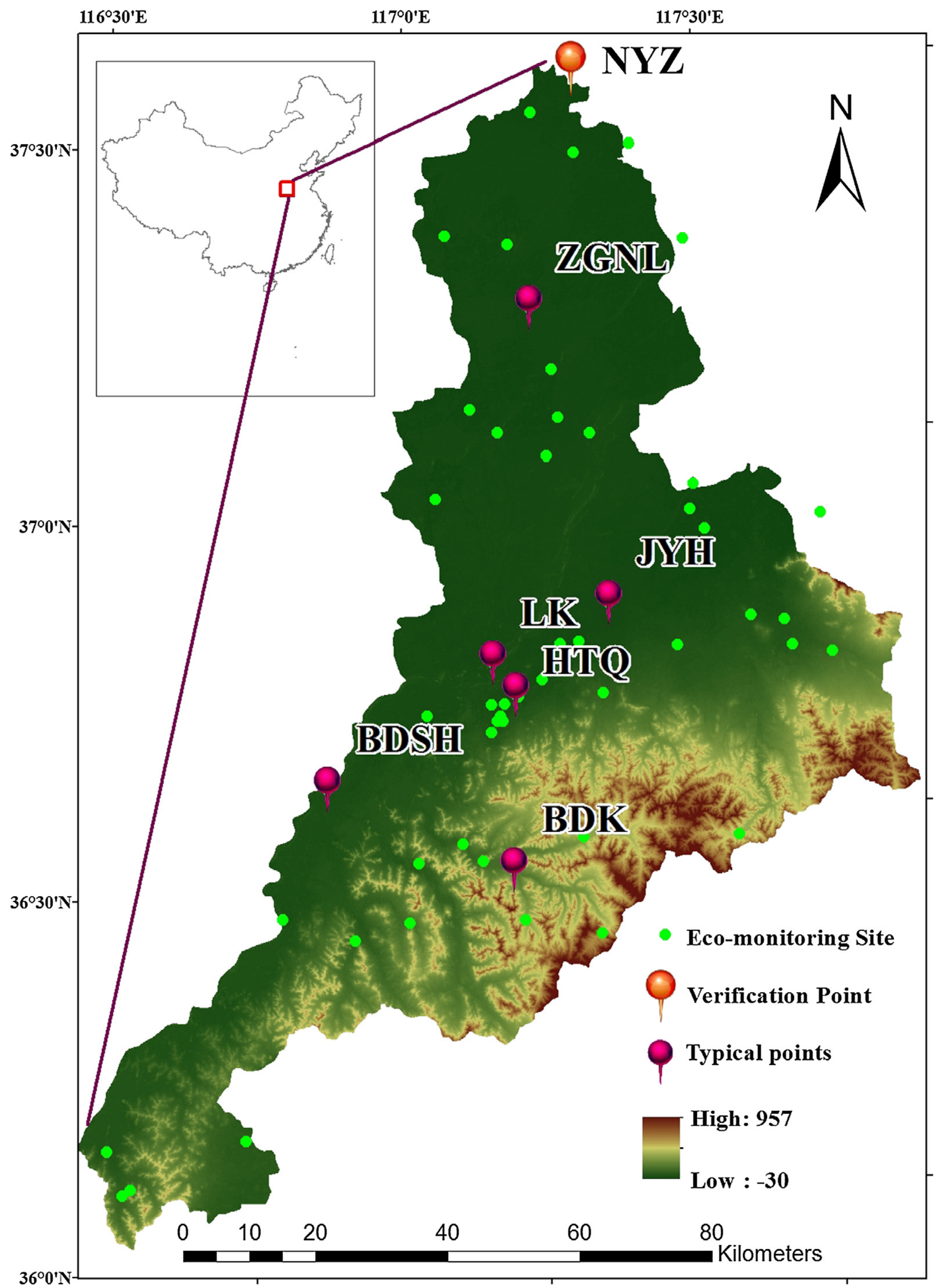

Fig. 1. Study area and the monitoring points.

3. Method

3.1. Using UAV to determine channel cross-section

Channel sections are critical parameters for calculating e-flow and are usually acquired by the traditional, artificial measurement method. In this study, UAV was employed to acquire high-resolution stereoscopic images, which were used to obtain high-resolution topographic data, and the channel section was then calculated using the 3D Analyst module of ArcGIS 10.4.

The stereoscopic images were processed by the rapid and automatic professional processing software Pix4Dmapper (https://pix4d.com/). Image treatment includes data importing, initial processing, point cloud encryption, digital orthophoto map (DOM) generation, and digital surface model (DSM) generation (Turner et al., 2014; Ruzgienė et al., 2015).

UAV images can only acquire above ground topography information; it is difficult to obtain underwater topography. To acquire a full cross-section, above ground topography was confirmed by UAV and underwater topography was fitted using the measured water depth and cross-section. In a natural river channel, the

Table 1
Fish species recorded in Jinan City during the eight field campaigns from 2014 to 2016.

No.	Species	No.	Species
1	*Opsariichthys bidens Gunther*	30	*Rhinogobio nasutus*
2	*Carassius auratus*	31	*Cirrhinus molitorella*
3	*Pseudorasbora parva*	32	*Oncorhynchus mykiss*
4	*Mastacembelus aculeatus*	33	*Tridentiger trigonocephalus*
5	*Hemiculter leucisculus*	34	*Siniperca scherzeri*
6	*Sarcocheilichthys nigripinnis*	35	*Gobio rivuloides*
7	*Gnathopogon imberbis*	36	*Erythroculter ilishaeformis*
8	*Misgurnus anguillicaudatus*	37	*Sphyraenus*
9	*Monopterus albus*	38	*Abbottina rivularis* Basilewsky
10	*Huigolio chinssuensis*	39	*Rhodeus lighti* Wu
11	*Rhodeus sinensis* Gunther	40	*Rhodeus ocellatus* Kner
12	*Ctenogobius brunneus*	41	*Ctenogobius giurinus* Rutter
13	*Hypseleotris swinhonis*	42	*Culter erythropterus* Basilewsky
14	*Ctenogobius giurinus* (Rutter)	43	*Channa argus* Cantor
15	*Perccottus glenii*	44	*Macropodus chinensis* Bloch
16	*Lefua costata* Kessler	45	*Squalidus wolterstorff* Regan
17	*Ctenogobius cliffordpopei*	46	*Saurogobio gymnocheilus* Lo
18	*Pelteobagrus fulvidraco*	47	*Pseudobagrus emarginatus* Regan
19	*Piceus*	48	*Culter alburnus* Basilewsky
20	*Ctenopharyngodon idellus*	49	*Acheilognathus chankaensis* Dybowsky
21	*Paramisgurnus dabryanus* Sauvage	50	*Cobitis sinensis* Sauvage et Dabry
22	*Silurus asotus* Linnaeus	51	*Pseudolaubuca engraulis* Nichols
23	*Cyprinus carpio* Linnaeus	52	*Protosalanx hyalocranius* Abbott
24	*Pseudorasbora fowleri* Nichols	53	*Saurogobio dabryi*
25	*Clarias fuscus*	54	*Sinibrama wui*
26	*Oryzias latipes*	55	*Pseudobagrus tenuis*
27	*Lateolabrax japonicus*	56	*Aristichthys nobilis*
28	*Spualiobarbus curriculus*	57	*Hypophthalmichthys molitrix*
29	*Hypophthalmichthys molitrix*	58	*Plagiognathops microlepis*

cross-sections can be divided into four types: circular arc, box culvert, trapezoid, and "V" shape (Liu et al., 2007). In this study, circular arc cross-sections include JYH and ZGNL, box culvert includes BDK and HTQ, and "V" shape includes BDSH and LK. The underwater topography can be generalized as shown in Table 2.

3.2. Determination of dominant fish species

Abundance and biomass are fundamental indices for biological monitoring. The two indices often rank differently, which makes it difficult to objectively assess the dominance or importance of a species in a community (Liu et al., 2011). To overcome this, Liu et al. (2011) combined them into one index using Eq. (1).

$$I_{importance} = \omega_1 PCT_{abundance} + \omega_2 PCT_{biomass} \tag{1}$$

where "Importance" stands for the dominance of a species and $PCT_{abundance}$ and $PCT_{biomass}$ refer to the ratio of the species' abundance and biomass to the total for the communities, respectively. The larger the "Importance," the more the species contributes to its community, and the more important it is in the community. Parameters ω_1 and $\omega_2$are the weightings of abundance and biomass, $\omega_1 + \omega_2 = 1.0$, which are determined in our research (Zhao et al., 2015a) as 0.41 and 0.59, respectively.

3.3. Determination of ecological velocity and water depth for AEHRA

The habitat suitability index (HSI), varying between 0 and 1, is an effective indicator quantifying the response of a species to a set of habitat attributes (Ban et al., 2009; Vadas and Orth, 2001; Vismara et al., 2001). It is widely used to indicate the degree of preference of a species to various habitats (Leclerc et al., 2003; Ahmadi-Nedushan et al., 2006). Highly preferred habitats usually have high HSI values. Previous methods for determining HSI typically target one species (Wakeley, 1988; Tikkanen et al., 2007; Gong et al., 2012; Zohmann et al., 2013) instead of multiple species or a community, which makes it difficult to estimate the synthetic effect of a habitat factor on the ecosystem community (Zhao et al., 2015b). For this purpose, Zhao et al. (2015b) developed a new multispecies-based HSI (MHSI) to estimate the multi-species response to habitat environmental factors (Eq. (2)). In this method, the accumulated suitability probability, based on the preference of multiple dominant species (Eq. (5)), is used to represent the effect of habitat factors on the community at a certain gradient.

$$MHSI_k = \sum_{i=1}^{I} \frac{p_{ki}}{I} \quad \text{with} \quad p_{ki} = \frac{n_{ki}}{N_i} \tag{2}$$

where k stands for the kth gradient of a certain habitat environmental factor, e.g., flow velocity, water depth, $k = 1, \ldots K$; K is the total number of gradients along the habitat factor; i stands for the ith dominant species ($i = 1, \ldots, I$); I is the total number of the dominant species; n_{ki} is the abundance of the ith species in the kth gradient of the habitat factor; N_i is the abundance of the ith species in all gradients of the habitat factor, $N_i = \sum_{k=1}^{K} n_{ki}$; p_{ki} is the suitability probability of the ith species in the kth gradient; $MHSI_k$ is the multi-species based HSI, i.e., the suitability probability of all dominant species in the kth gradient, varying between 0 and 1.

Biodiversity index and IBI (Index of Biotic Integrity) are often used as indicators for ecosystem health (Weaver and Shannon, 1949; Wu et al., 2014; Zhao et al., 2015 b). The goal of e-flow monitoring is to maintain the health of river ecosystems. Therefore, the biodiversity index and IBI were introduced to this study to help determine the ecological velocity and water-depth for AEHRA.

3.4. Calculating e-flow and supplying-rate

3.4.1. E-flow assessment (Q_E) using AEHRA

The basis of AEHRA is the determination of ecological velocity (V_E). The velocity requirements of fish species vary by season, which can be determined using the MHSI (Eq. (2)). Having obtained the V_E, e-flow, Q_E, in the river section can be estimated using

Table 2
Relationship between cross-section and hydraulic radius (Liu et al., 2007).

Shape	Area (A)	Wetted perimeter (P)	Hydraulic radius (R)	Site
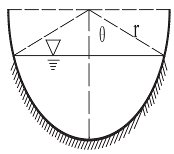 **Circular arc**	$A = \frac{1}{2}(\theta - \sin 2\theta)\cdot r^2$	$P = 2\theta \cdot r$	$R = \frac{A}{P} = \frac{1}{2}[1 - \frac{\sin 2\theta}{\theta}]\cdot r$	JYH ZGNL
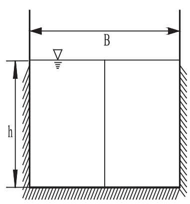 **Box culvert**	$A = B \cdot h$	$P = B + 2h$	$R = \frac{B \cdot h}{B+2h}$	BDK HTQ
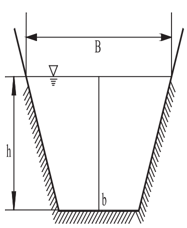 **Trapezoid**	$A = \frac{1}{2}(B+b)\cdot h$	$P = b + \sqrt{(B-b)^2 + 4h^2}$	$R = \frac{(B+b)\cdot h}{2b+2\sqrt{(B-b)^2+4h^2}}$	
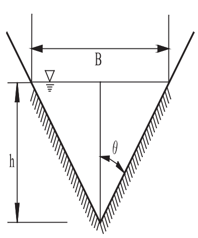 **"V" shape**	$A = \frac{1}{2}B \cdot h$	$P = \sqrt{B^2 + 4h^2}$	$R = \frac{B \cdot h}{2\sqrt{B^2+4h^2}}$	BDSH LK

AEHRA (Eq. (3)). Cross-sectional data used as essential input variables were rapidly retrieved using the method in Section 3.1.

$$Q_E = \frac{1}{n} R_E^{\frac{2}{3}} A_E J^{\frac{1}{2}} \quad \text{with} \quad R_E = n^{\frac{3}{2}} V_E^{\frac{3}{2}} J^{-\frac{3}{4}} \quad (\text{Liu et al., 2011}) \tag{3}$$

Q_E is e-flow in $m^3{\cdot}s^{-1}$; R_E refers to the watercourse hydraulic radius (ratio between cross-sectional flow area and its wetted perimeter) corresponding to V_E in m; A_E is the flow area for e-flows in m^2; n is a dimensionless roughness value; and J is the hydraulic slope in%.

3.4.2. E-flow supplying-rate calculation

For calculating e-flow supplying-rate, a supplying-rate evaluation model was built combining minimum e-flow (Q_E_min) and measured flow (Eq. (4)). If the supplying-rate is greater than 1, there is no lack of water; if the supplying-rate is less than 1, the flow cannot meet the requirements of Q_E_min. The water deficit rate is calculated using Eq. (5).

$$\text{Supplying-rate} = \text{Measured flow}/Q_E\text{\_min} \tag{4}$$

$$\text{Water deficit rate} = (\text{Measured flow} - Q_E\text{\_min})/Q_E\text{\_min} \tag{5}$$

$$|\text{Supplying-rate}| + |\text{Water deficit rate}| = 1 \tag{6}$$

4. Results

4.1. Inverting river cross-sections using UAV

Through the method described in Section 3.1, cross-sections were fitted using UAV (Unmanned Aerial Vehicle) and measured data. Fig. 2 clearly shows that circular arc cross-sections include JYH (Juyehe) and ZGNL (Zhanggongnanlin), box culvert cross-sections include BDK (Bingdukou) and HTQ (Huangtaiqiao), and "V" shape cross-sections include BDSH (Beidashahe) and LK (Luokou), highlighting the rapid and flexible acquisition of underwater topography using this method.

4.2. Suitable flow velocity and water depth of dominant fish species

As successful spawning and survival during the early life stages of fish often dictate the strength of subsequent cohorts (Trippel and Chambers, 1997), understanding the influence of natural flow regimes on the early life stages of fish is vital to protect fish populations in flow altered rivers (Balcombe et al., 2006). Flow velocity is one of the most important variables determining the likelihood of successful fish spawning (Nelson and Lieberman, 2002; Liu et al., 2011). The MHSI (Eq. (2)) is used to estimate the responses of fish communities to habitat environmental factors to determine the optimum flow velocity and water depth as inputs for AEHRA (Fig. 3).

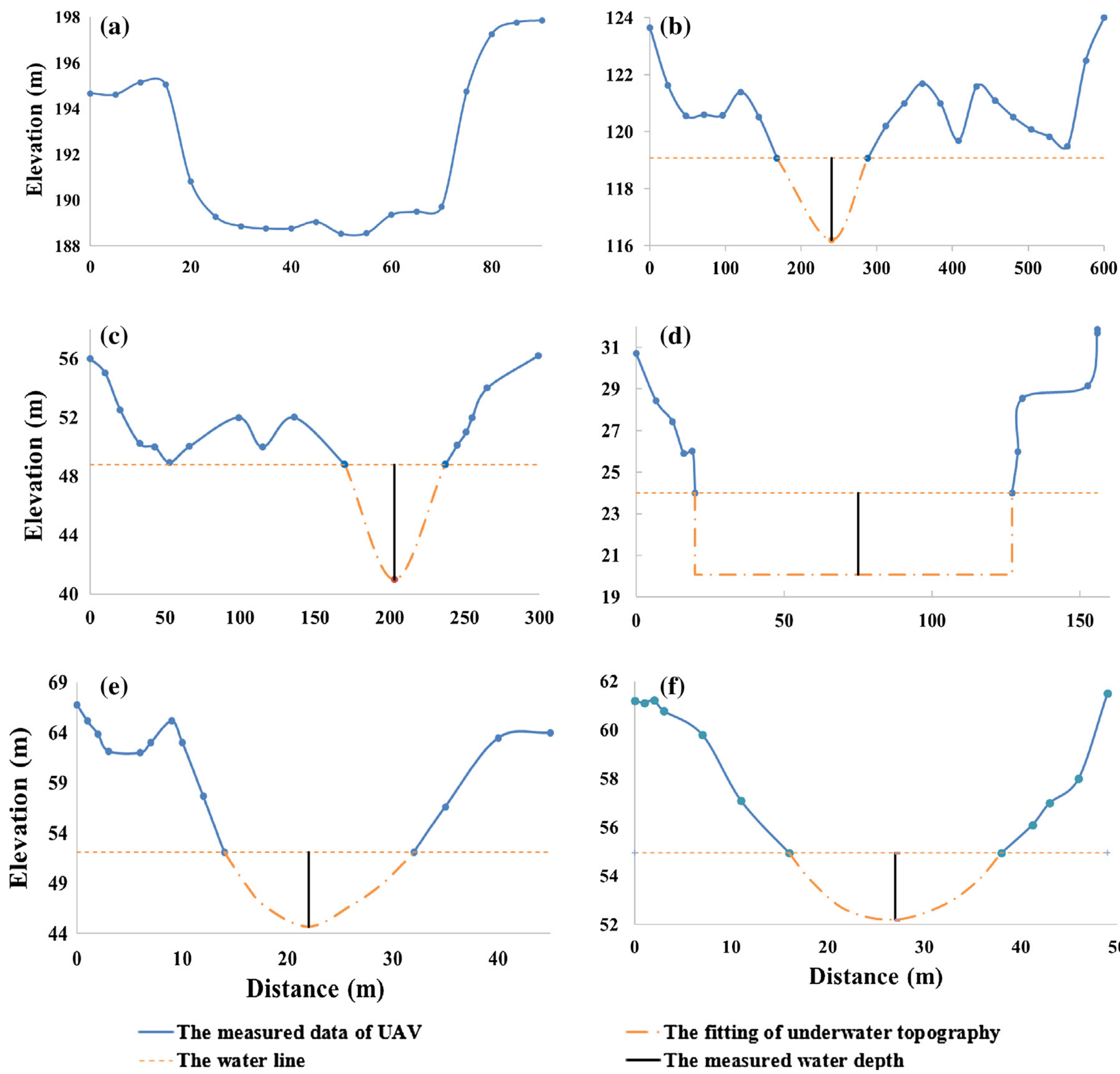

Fig. 2. River cross-sections for different monitoring stations. (a) BDK (dried up), (b) BDSH, (c) LK, (d) HTQ, (e) ZGNL, and (f) JYH.

Regarding flow velocity, the dominant fish species of HTQ survive better under a low velocity of 0.2 m/s; the dominant fish species of LK are slightly more adaptable to flow velocity, preferring approximately 0.15–0.18 m/s. The flow velocity of the other sites shows little influence on the survival of fish communities. Regarding water depth, fish communities in BDK, ZGNL, and JYH prefer shallow water. In BDSH, fish communities survive in a water depth interval of 0.3–0.5 m. In LK, the suitable water depth is over 1 m or between 0.3 and 0.5 m. In HTQ, fish communities prefer a water depth interval of 0.3–0.7 m.

To ensure the best chances of egg survival, there are four types of egg specially adapted to the surrounding environment: floating, pelagic (semi-floating), demersal, and adhesive (Zhao et al., 2008). The information in Table 3 comes from the literature (He and Song, 1996; Li et al., 2006; Wang, 1992) and field sampling data.

Fish that can produce pelagic eggs have a higher demand on flow velocity. As the fish hatch in a pelagic state, the larval hatching rate will be reduced when the eggs sink to the bottom due to low velocity or static water. For floating eggs, the flow velocity demand is generally less than 0.95 m/s, and the water depth demand is generally less than 2 m. For adhesive eggs, the requirements for laying eggs are lower, both water level and aquatic plants control the spawning conditions. Therefore, limited uplift and a constant water level can result in a larger spawning area, which benefits the spawning conditions for fish that lay adhesive eggs (Zhao et al., 2008). Table 3 shows the detailed spawning conditions of the dominant fish species.

4.3. Biodiversity and IBI of the fish community in Jinan city

Both water depth and flow velocity used in this study are actual values from fish community monitoring, and they can only partly reflect the water depth and flow velocity demands of fish communities. In this study, we also analyze suitable water depth and flow velocity by combining biodiversity (H) and the habitat adaptability index (IBI) (Fig. 4).

In Fig. 4, flow velocity and water depth should be equal to or greater than 0.11 m/s and 0.60 m, respectively, to ensure the two indexes are greater than the average value for Jinan. According to these flow velocity and water depth values, the ecological flow velocity (V_E) and ecological water depth (H_E) values for 2016 were calculated by combining the suitable flow velocity and water depth from Section 4.2 and considering the spawning water depth and flow velocity demands of fish communities, which are as follows.

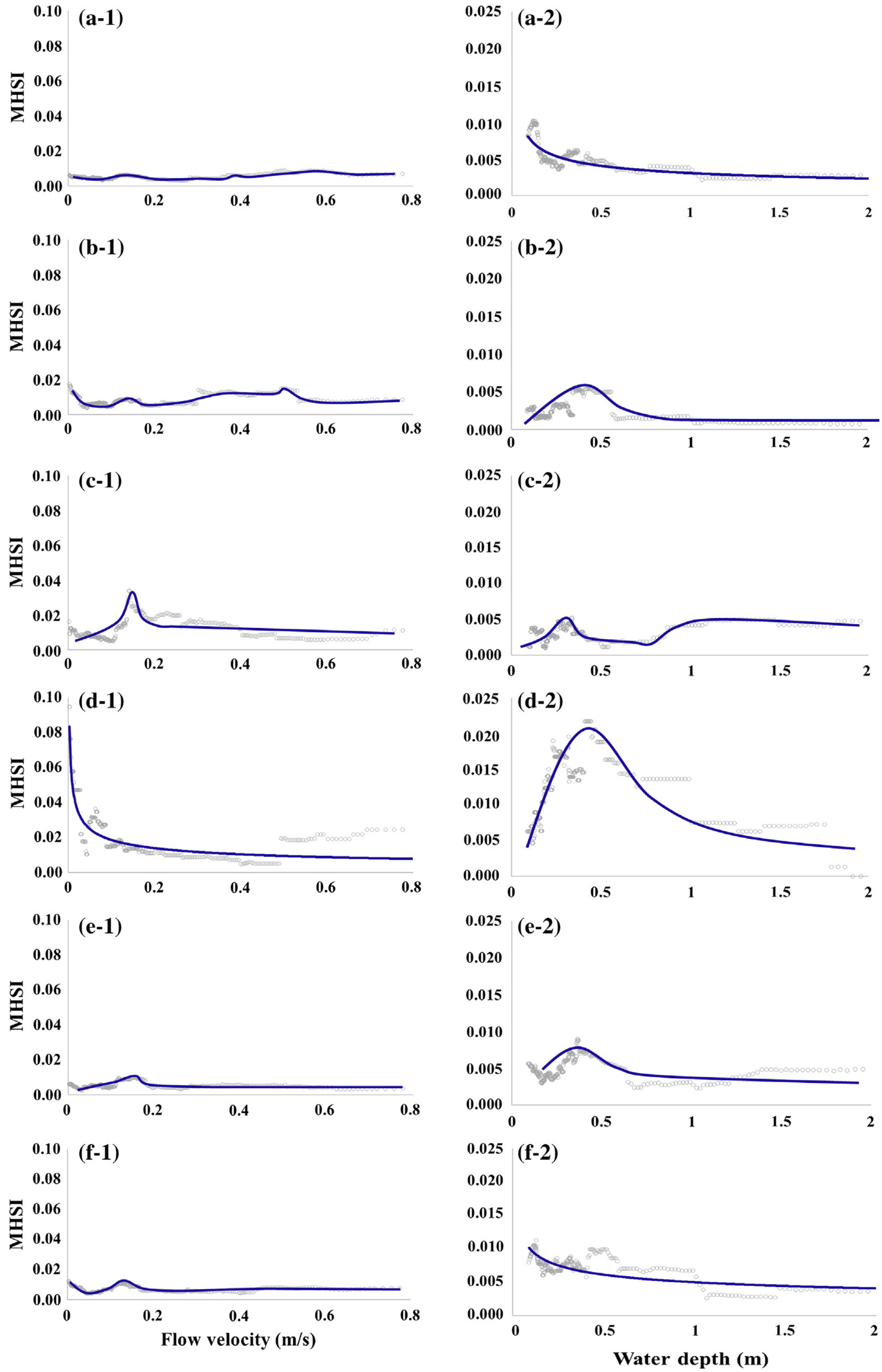

Fig. 3. Fitted curves for suitable flow velocity and water depth of dominant fish species: a–f represent sites BDK, BDSH, LK, HTQ, ZGNL, and JYH, respectively, and numbers 1 and 2 represent the flow velocity and water depth, respectively.

- In BDK, the H_E of the spawning period is greater than 0.8 m in 4 months of the year and greater than 1.5 m in 8 months, and the H_E is greater than 0.6 m in non-spawning months. The V_E is greater than 0.3 m^3/s in 8 months and 0.11 m^3/s in the remaining months.
- In BDSH, the H_E of the spawning period is greater than 0.8 m in 4–6 months of the year and greater than 1.5 m in 7 months, and the H_E is greater than 0.6 m in non-spawning months. Annual V_E is greater than 0.11 m^3/s.

Table 3
Spawning demands of dominant fish species.

Dominant fish species	Spawning time (month)	Spawning type	Water depth demand (m)	Flow velocity demand (m/s)
Saurogobio dabryi	3–4	Floating	0.2–1.0	0.027–0.95
Oryzias latipes	5–6	Floating	0.1–0.3	0.027–0.95
Spualiobarbus curriculus	5–7	Floating	1.5–2.0	0.027–0.95
Channa argus Cantor	4–7	Floating	0.2–1.0	0.027–0.95
Opsariichthys bidens Gunther	6–8	Pelagic	1.5–4.0	0.304–1.8
Cobitis sinensis Sauvage et Dabry	5–7	Pelagic	0.1–0.5	0.304–1.8
Carassius auratus	4–5	Adhesive	0.8–1.2	0.022–1.04
Pseudorasbora parva	4–6	Adhesive	0.3–0.4	0.001–1.5
Misgurnus anguillicaudatus	4–5	Adhesive	0.1–0.2	0.002–1.04
Abbottina rivularis Basilewsky	4–5	Adhesive	0.1–0.2	0.002–1.04
Paramisgurnus dabryanus Sauvage	4–5	Adhesive	0.1–0.2	0.002–1.04
Hemiculter leucisculus	5–7	Adhesive	0.5–10	0.001–1.5
Sinibrama wui	4–5	Adhesive	0.2–1.0	0.022–1.04
Acheilognathus chankaensis Dybowsky	5–6	Adhesive	0.8–1.2	0.002–1.04
Rhodeus lighti Wu	4–6	Adhesive	1.5–2.5	0.002–1.04
Cyprinus carpio Linnaeus	4–5	Adhesive	0.8–1.2	0.022–1.04
Rhodeus sinensis Gunther	4–6	Adhesive	1.5–2.5	0.022–1.04
Ctenogobius brunneus	4–5	Adhesive	0.1–0.3	0.002–1.04

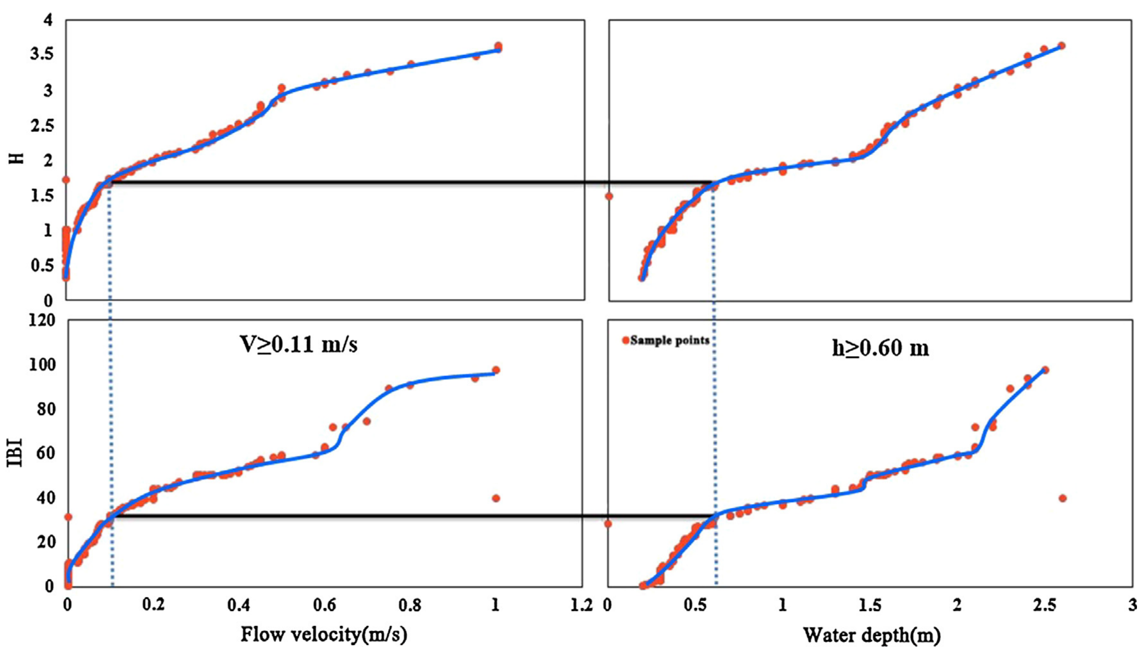

Fig. 4. Biodiversity (H) and IBI indexes.

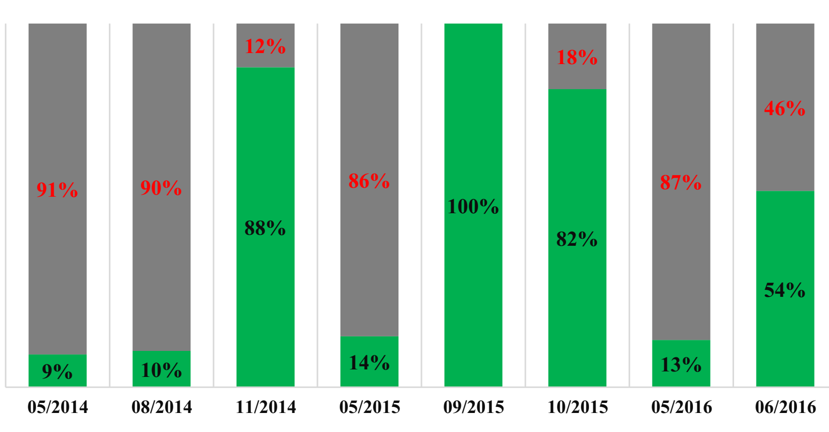

Fig. 5. E-flow satisfaction and shortage ratio for BDK.

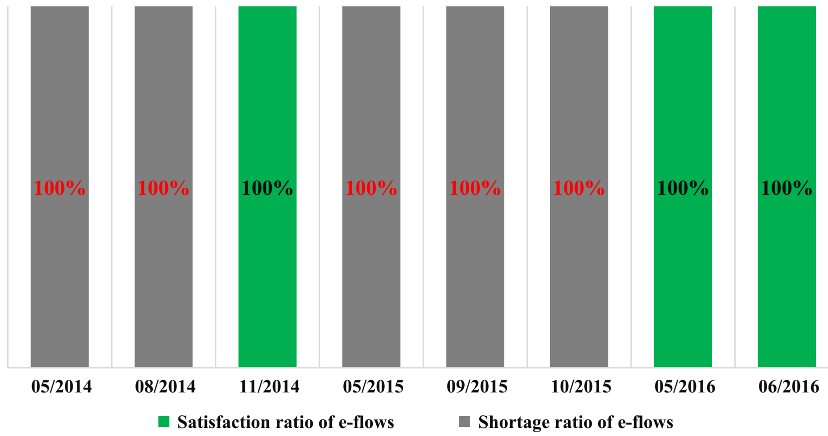

Fig. 6. E-flow satisfaction and shortage ratio in BDSH.

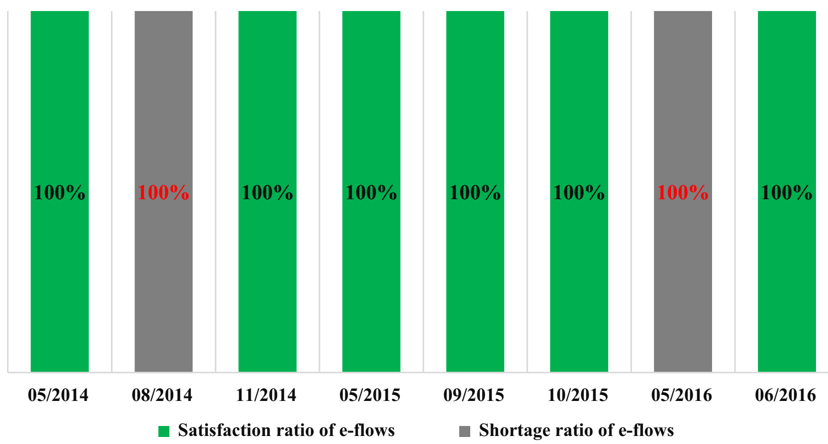

Fig. 7. E-flow satisfaction and shortage ratio in ZGNL.

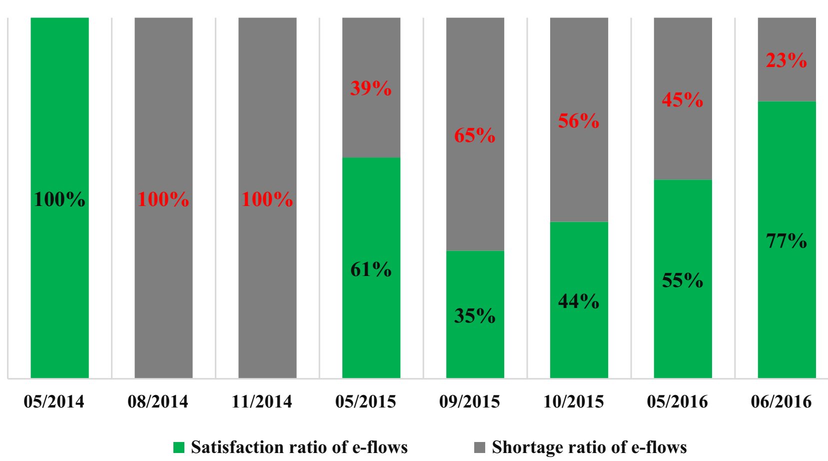

Fig. 8. E-flow satisfaction and shortage ratio in JYH.

- In LK and HTQ, the H_E and V_E are respectively greater than 0.6 m and 0.11 m^3/s all year round.
- In ZGNL and JYH, the H_E of the spawning period is greater than 0.8 m in 4–5 months of the year, and the H_E is greater than 0.6 m in non-spawning months. The annual V_E is greater than 0.11 m^3/s.

The above results indicate the demand for flow velocity and water depth during the fish spawning period in typical river sections. Locations where H and IBI were considered show values greater than the average value for Jinan, but the average flow velocity and water depth values were generally achieved during the non-spawning period. For the Jinan basin, the V_E is equal to or greater than 0.11 m/s, and the H_E is greater than 0.6 m.

4.4. Calculating e-flow and supplying-rate

With the ecological flow velocity and water depth determined in Section 4.3, e-flows were calculated using AEHRA, described in Section 3.4, and the relationships with e-flow supply were quantitatively evaluated by combining the measured water depth and supplying-rate evaluation model from Section 3.4. The calculation results show that study points can be divided into two types: one where all e-flows are satisfied, such as LK and HTQ; and one where e-flows are partly satisfied, such as BDK, BDSH, ZGNL, and JYH. LK and HTQ have no water deficit because of higher flow velocity and water depth all year round. Other study points lack water during some months because of intense human activities. Here, we quantitatively evaluated the e-flow supplying-rate relationship using the evaluation model in

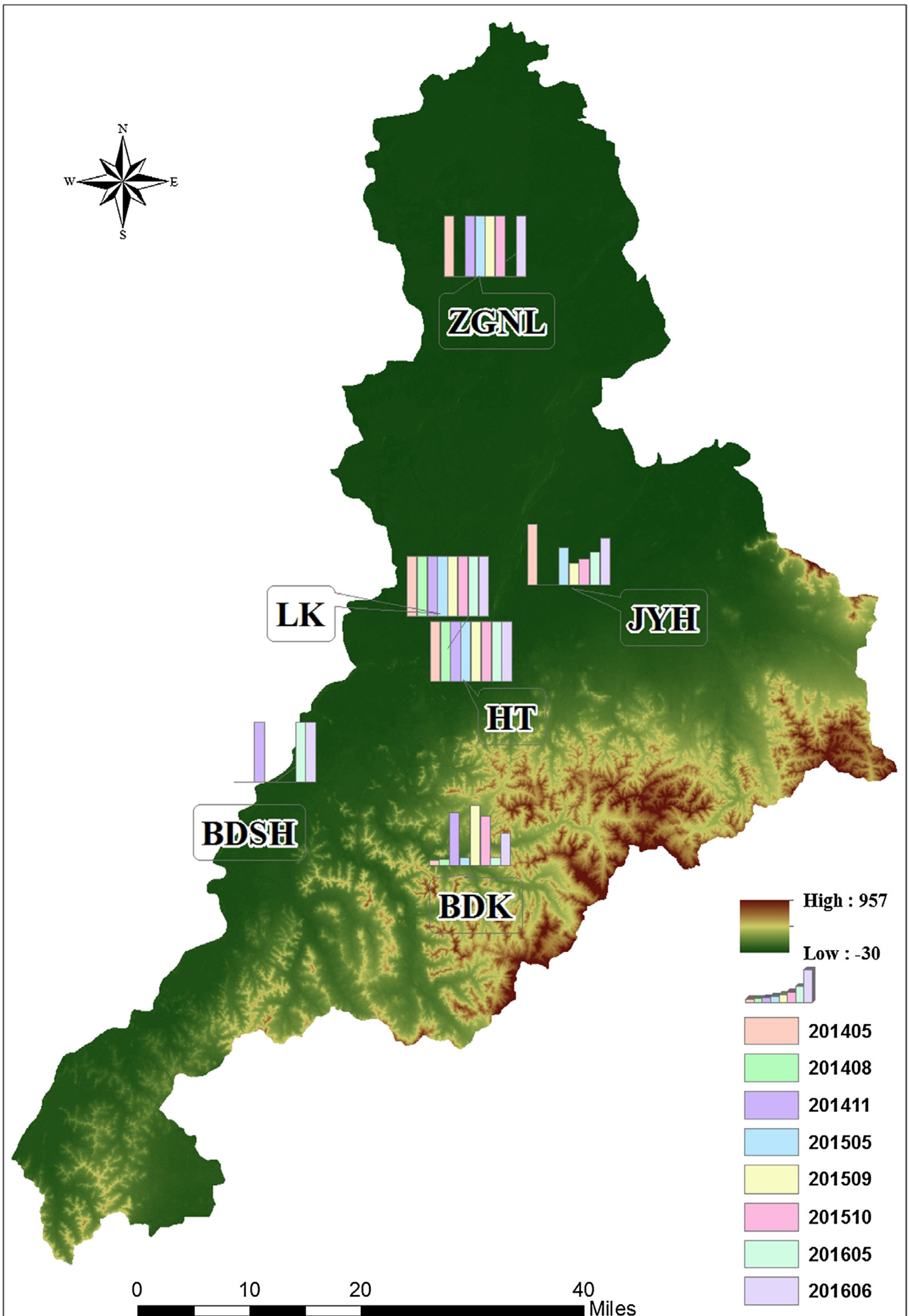

Fig. 9. Spatial distribution of the satisfaction ratio of typical e-flows.

Section 3.4, which can provide reliable scientific input for water conservation projects.

4.4.1. BDK

The flow at BDK depends on an upstream reservoir and rainfall runoff. Fig. 5 shows that the e-flow supplying-rate and shortage ratio differ throughout the year; e-flow values are lower in spring and winter and higher in summer and autumn. Only one of the eight field sampling periods shows no water shortage because the upstream reservoir was sluiced during that month. Overall, the e-flows lack water all year around because regular dams (every 300–500 m) intercept the water upstream. For the sustainable development of a healthy ecosystem in BDK, we advise unified management of basin water resources.

4.4.2. BDSH

Of the eight field sampling periods (Fig. 6), there is an e-flow satisfaction ratio of 100% in three, and these benefit from the healthy development of the channel ecosystem. For the other five samples, the e-flow shortage ratio is 100%, indicating that the channel is dry and the channel ecological health is threatened. We conclude that the year of 2015 was dry because there is no water in the three field sampling campaigns of 2015. This is the consequence of excessive water use by agricultural irrigation.

4.4.3. ZGNL

ZGNL is located in the north of study area, its main land use is plowland. Many artificial rivers were constructed for irrigation by local departments. Of the eight field sampling campaigns (Fig. 7), the e-flow shortage ratio is 100% in two. In general, e-flows occur mainly in the fifth month of each year, and the intervening period is for irrigation. The flow volume in north Jinan mainly depends on diversion works and rainfall. Diversion water volume should be controlled wisely during irrigation periods because too much of diversion will inevitably influence the ecological health of the river channel.

None of the eight field sampling campaigns of JYH, except one (Fig. 8), completely satisfy the minimum e-flow. The river is dried up in the second and third sampling, which seriously affects healthy development of the river ecosystem. The satisfaction of e-flows is generally less than 100% in the long term, and this not only affects the growth and breeding of river biota, but also hinders the sustainable development of an ecological healthy channel.

After the analysis of individual sampling locations, their spatial distribution was comprehensively considered. We found that flow volume is essentially equal to the e-flows in rivers close to the Yellow and Xiaoqing Rivers (Fig. 9), and the ecosystem of these rivers is healthy. In the river networks of south Jinan, the upstream cannot always satisfy the minimum e-flow requirements, but the downstream generally satisfies the minimum e-flow requirements. In the north, there are artificial rivers to irrigate, and the flow volume produced by rainfall hardly satisfies the minimum e-flow and irrigation water requirements. Therefore, water from the Yellow River should be introduced by diversion works to rectify the water shortage.

5. Discussion

5.1. Validation of cross-sections determined by UAV

Traditional artificial measurement methods of channel cross-sections, such as Total Station and Level Gage, require large amount of time, materials, and power, and can be dangerous when one crosses the large-flow river with handing prism. In topographic surveys, 3D models of precipitous topography can be built to monitor displacement (Pierzchala et al., 2014; Clapuyt et al., 2016) and research the process of soil erosion (Neugirg et al., 2016) using stereoscopic images of UAV, and UAV can also be used to explore the melting processes of seasonal polar glaciers (Kraaijenbrink et al., 2016). Previous studies indicate that UAV-based topographic survey precision can reach centimeter levels (Anderson and Gaston, 2013; Zarco-Tejada et al., 2014; Neugirg et al., 2016). In this research, the channel cross-sections were measured by UAV, and the results were verified to ensure reliability using field data measured by the Total Station method.

The precision of two study locations were verified using the Total Station method (Fig. 10). The relative root mean square error (RMSE) was used to evaluate the precision of the UAV method.

$$RMSE = \sqrt{\frac{\sum_{i=1}^{n}(X_{obs,i} - X_{model,i})^2}{n}} \tag{7}$$

The results show that the RMSE between UAV data and field data is 24 cm in BDK, where the channel is dried up (Fig. 11). The RMSE between UAV data and field data in ZGNL is 23.6 cm above the water, where the channel is influenced by the water,

Fig. 10. Channel cross-sections measured by the Total Station method.

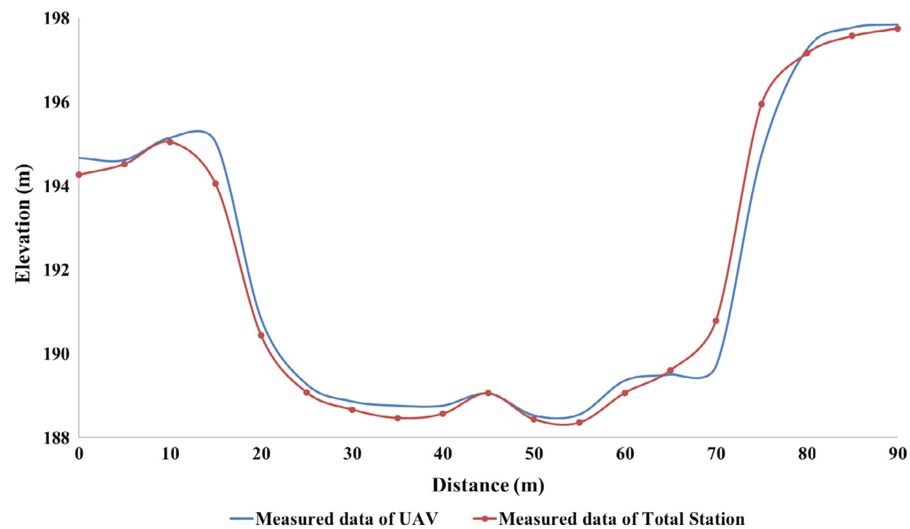

Fig. 11. Channel cross-section measured by UAV and the Total Station method for BDK.

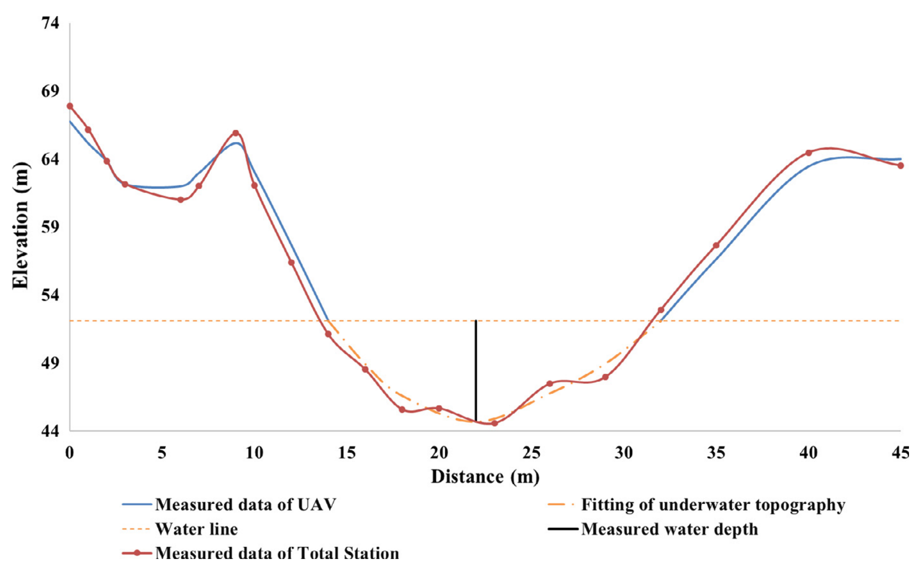

Fig. 12. Channel cross-section measured by UAV and the Total Station method for ZGNL.

but below the water topography was not measured because it is very difficult for the electromagnetic wave to penetrate the water surface. The topography below the water surface was fitted by combining the measured water depth and the channel section shape, and the resulting total RMSE is 24.8 cm, considering the topography above the water measured by UAV (Fig. 12). These results indicate that the RMSE for UAV determined channel cross-sections is less than 0.25 cm, which makes up 3–5% of the river's depth. This fully meets the precision requirements of e-flow calculations.

5.2. Influence of hydrological parameters on fish communities

In terms of the aquatic ecosystem, one of the most obvious and unacceptable effects of anthropogenic activities is the collapse of the riverine fish community due to uninformed river regulation strategies that lead to reduced flow and a corresponding decrease in water quality. Stream flows that are adequate to maintain fisheries are usually sufficient to maintain macro-invertebrates and other aquatic life (Doledec et al., 2015). Fish communities are thus considered effective indicators of ecosystem health. As successful spawning and survival during the early life stages of fish often dictate the strength of subsequent cohorts, understanding the influence of natural flow regimes on the early life stage of fish is vital

Table 4
Calculation results of e-flow in NYZ using AEHRA.

Month	Min e-flow (m^3/s)	Min ecological water level (m)	Min ecological water depth (m)
1	0.248	−0.59	0.91
2	0.248	−0.59	0.91
3	0.248	−0.59	0.91
4	0.248	−0.59	0.91
5	8.978	−1.38	2.88
6	8.978	−1.38	2.88
7	0.248	−0.59	0.91
8	0.248	−0.59	0.91
9	0.248	−0.59	0.91
10	0.248	−0.59	0.91
11	0.248	−0.59	0.91
12	0.248	−0.59	0.91

Table 5
Calculation results of e-flow in NYZ using the Tennant method.

Habitat quality	Max	Optimum	Excellent	Very	Good	Medium	Bad
Flow during general water phase (m^3/s)	2.58	1.29	0.516	0.387	0.258	0.129	0.129
Flow during fish spawning period (m^3/s)	2.58	1.29	0.774	0.645	0.516	0.387	0.129

for protecting fish populations in flow-altered rivers (Balcombe et al., 2006). Flow alteration also plays an important role in fish body shape changes, periodic life-history strategy, and fish community structure (Meyers and Belk, 2014; Lamouroux and Olivier, 2015; Pool and Olden, 2015).

As well as flow volume, other hydrological features such as water depth and flow velocity are essential for maintaining biodiversity and ecosystem integrity. A change in flow volume or flow velocity can easily alter the distribution of aquatic organisms and species composition. These features mainly alter hydrological processes and influence the water ecosystem (Cui et al., 2009).

In the above researches, many authors were aware of the importance of flow velocity and water depth on fish species, but few quantitative results were given closely related to the health of fish communities. Differently from the previous researches, two indices of biodiversity (H) and integrated biotic index (IBI) were used in this study as indicators of the health of fish communities, and the dominant fish species were selected using field data. The average flow velocity and water depth relating closely to the health of fish communities were calculated quantitatively as flow velocity (equal to/greater than 0.11 m/s) and water depth (greater than 0.8 m). The two threshold values not only are extremely significant to the remediation of river health and e-flows assessment in the study area but also could be important references for e-flow assessment in other areas across the world.

5.3. Evaluating the reliability of the method

The Tennant method was used to verify the reliability of the e-flow method proposed in this study. The NieYingZha (NYZ) station, with abundant historical data, was selected to verify the reliability, because the Tennant method is based on historical hydrological data. The e-flow was calculated for the downstream part of NYZ using AEHRA (Table 4) and the Tennant method (Table 5).

The AEHRA results are classed between Medium and Good during the non-spawning period, but are significantly larger during the spawning period. This phenomenon is due to the influence of dams causing large changes in flow volume. Sometimes, the river has no water because of the upstream dams being closed, and this makes calculating the e-flow by the Tennant method difficult. In addition, the Tennant method does not consider water depth and flow velocity, which are important parameters for the habitat of aquatic life. However, the AEHRA effectively considers the effect of dams on e-flow, especially the water depth and flow volume demands of fish during spawning periods.

On the whole, the AEHRA method effectively takes into account changes in biological life, as well as the specific demands for velocity, water depth, and flow during important periods; e.g., spawning and migration. When used as a method to calculate e-flow, it can help effectively protect the healthy development of river ecosystems.

6. Conclusions

The calculation of e-flow and supplying-rate for dominant fish species is crucial for evaluating the health of a channel ecosystem. This study presents a new method for rapid e-flow assessment based on UAV and AEHRA. E-flows at several locations in Jinan were calculated and their satisfaction ratios were analyzed. The results show that:

(1) The RMSE of the UAV-measured channel cross-sections was less than 0.25 m, which constitutes 3–5% of the river depth. This fully meets the precision demands of e-flow calculations.
(2) Flow velocity and water depth in the Jinan basin was equal to or greater than 0.11 m/s and greater than 0.6 m, respectively.
(3) Using the Tennant method, the AEHRA results are medium to good in the non-spawning period but significantly larger in the spawning period. The AEHRA method can effectively consider changes in biological life and specific velocity, water depth, and flow demands during certain periods, such as spawning and migration periods. This e-flow calculation method can effectively promote the overall healthy development of river ecosystems.
(4) Flow volume meets e-flow requirements in rivers close to the Yellow and Xiaoqing Rivers, and these river ecosystems are healthy. In the river networks of south Jinan, the upstream cannot always satisfy the minimum e-flow requirements, but the downstream generally satisfies the minimum e-flow requirements. In the north, there are artificial rivers to irrigate, and the flow volume produced by rainfall hardly satisfies the minimum e-flow and irrigation water requirements. Therefore, water from the Yellow River should be introduced by diversion works to rectify the water shortage.
(5) The survey locations can be divided into two types: one where e-flows are satisfied, such as LK and HTQ, and the other where e-flows are partly satisfied, such as BDK, BDSH, ZGNL, and JYH. LK and HTQ do not lack water because of a higher flow velocity and water depth all year round. Other locations lack water in some months of the year because of intense human activities. In this research, we quantitatively evaluated the e-flow supplying-rate relationship, the results of which can provide reliable scientific advice for water conservation projects.

Overall, the usage of UAV to acquire channel parameters in this study provided a novel prospect for rapid e-flow assessment. The method can effectively promote research progress into basin e-flow, and provide an important reference for global e-flow monitoring. As such, the protection and restoration of aquatic ecosystems under intensive human activities at basin or larger scales turn time- and cost-effectively. All methodologies and according results could be important references for e-flow assessment in other areas across the world.

During data acquisition, the field sampling can be disturbed by human factors, which leads to unavoidable uncertainties. Therefore, the influence of human factors should be reduced to improve e-flow calculation precision in future research. Moreover, floods can modify cross-sections during a hydrological year and therefore effects of floods on results should be carefully considered for further investigations to further improve the precision of results.

Acknowledgements

We acknowledge the reviewers and editors for their valuable advice on improving the quality of this paper. We thank associate Professor Xuwang Yin from the Dalian Ocean University, as well as our colleagues from the Jinan and Dongying Survey Bureau of Hydrology, and Beijing Normal University for their support in funding the research and collaboration during field investigations. We would like to thank Editage for English language editing and also thank the PIX4D Company for their software, used in our study to process UAV images.

This research was jointly supported by the National Key Project for R&D (Grant numbers 2016YFC0402403 & 2016YFC0402409), the National Natural Science Foundation Program of China [Grant numbers 41271414 & 41471340], and the Program for Key Science and Technology Innovation Team in Shaanxi province [Grant number 2014KCT-27), China.

References

Ahmadi-Nedushan, B., St-Hilaire, A., Bérubé, M., et al., 2006. A review of statistical methods for the evaluation of aquatic habitat suitability for instream flow assessment. River Res. Appl. 22, 503–523.
Anderson, K., Gaston, K.J., 2013. Lightweight unmanned aerial vehicles will revolutionize spatial ecology. Front. Ecol. Environ. 11 (3), 138–146.
Aquilanti, L., Clementi, F., Nanni, T., Palpacelli, S., Tazioli, A., Vivalda, P.M., 2016. DNA and fluorescein tracer tests to study the recharge, groundwater flowpath and hydraulic contact of aquifers in the Umbria-Marche limestone ridge (central Apennines, Italy). Environ. Earth Sci. 75 (7), 1–17.
Armentrout, G.W., Wilson, J.F., 1987. An assessment of low flows in streams in northeastern Wyoming. In: US Geological Survey.
Balcombe, S.R., Arthington, A.H., Foster, N.D., Thoms, M.C., Wilson, G.G., Bunn, S.E., 2006. Fish assemblages of an Australian dryland river: abundance, assemblage structure and recruitment patterns in the Warrego River, Murray-Darling Basin. Mar. Freshwater Res. 57 (6), 619–633.
Ban, X., Li, D.M., Li, D., 2009. Application of habitat suitability criteria on spawnsites of Chinese sturgeon in downstream of Gezhouba Dam. Eng. J. Wuhan Univ. 42 (2), 172–177 (in Chinese).
Barbour, M.T., Gerritsen, J., Snyder, B., et al., 1999. Rapid Bioassessment Protocols for Use in Streams and Wadeable Rivers: Periphyton, Benthic Macroinvertebrates, and Fish. USEPA, Washington.
Chen, J., Xu, T., Fang, S., et al., 1987. Fishes in Qingling Mountain Area. Science Press, Beijing (in Chinese).
Chen, H., Yang, Y., Yu, S.W., Yang, Z.F., 2011. Study on ecological water demand based on assessment of ecosystem disturbance degree in the Baiyangdian Wetland. Acta Ecol. Sinica, 233–241.
Chen, Z.S., Chen, Y.N., Chen, Y.P., Li, W.H., 2012. Response of ecological water requirement to land use change in the newly reclaimed area of ili river basin in Xinjiang. J. Desert Res., 551–557
Clapuyt, F., Vanacker, V., Van, O.K., 2016. Reproducibility of UAV-based earth topography reconstructions based on Structure-from-Motion algorithms. Geomorphology 260, 4–15.
Comodi, G., Cioccolanti, L., Palpacelli, S., Tazioli, A., Nanni, T., 2011. Distributed generation and water production: a study for a region in central Italy. Desalin. Water Treat. 31 (1–3), 218–225.
Cui, Y., Zhang, Q., 2010. Advances in the theories and calculation methods of ecological water requirement. Scientia Limnologica Sinica 22 (4), 465–480.
Cui, B.S., Wang, C.F., Tao, W.D., et al., 2009. River channel network design for drought and flood control: a case study of Xiaoqinghe River basin, Jinan City. Chin. J. Environ. Manage. 90 (11), 3675–3686.
Doledec, S., Castella, E., Forcellini, M., Olivier, J.-M., Paillex, A., Sagnes, P., 2015. The generality of changes in the trait composition of fish and invertebrate communities after flow restoration in a large river (French Rhone). Freshw. Biol. 60 (6), 1147–1161.
Gong, C.X., Chen, X.J., Gao, F., Chen, Y., 2012. Importance of weighting for multivariable habitat suitability index model: a case study of winter-spring cohort of Ommastrephes bartramii in the Northwestern Pacific Ocean. J. Ocean Univ. China 11 (2), 241–248.
Gopal, B., 2016. A conceptual framework for environmental flows assessment based on ecosystem services and their economic valuation. Ecosyst. Serv. 21, 53–58.
He, X.F., Song, Z.B., 1996. The laying eggs and embryonic development of Saurogobio dabryi. J. Southwest Normal Univ.: Nat. Sci. Ed. 21 (3), 276–281.
Hong, Q.A., Meng, Q.B., Wang, P., et al., 2010. Regional aquatic ecological security assessment in Jinan. Chin. Aquat. Ecosyst. Health Manage. 13 (3), 319–327.
Joniak T., Kuczyńska-Kippen N., 2010. The chemistry of water and bottom sediments in relation to zooplankton biocenosis in small agricultural ponds. Oceanological and Hydrobiological Studies (abbrev. Oceanol Hydrobiol St) 39 (2): 85–96.
Kraaijenbrink, P., Meijer, S.W., Shea, J.M., Pellicciotti, F., De, J.S.M., Immerzeel, W.W., 2016. Seasonal surface velocities of a Himalayan glacier derived by automated correlation of unmanned aerial vehicle imagery. Ann. Glaciol. 57 (71), 103.
Lamouroux, N., Olivier, J.M., 2015. Testing predictions of changes in fish abundance and community structure after flow restoration in four reaches of a large river (French Rhone). Freshw. Biol. 60 (6), 1118–1130.
Leclerc, M., St-Hilaire, A., Bechara, J., 2003. State-of-the-art and perspectives of habitat modeling. Can. Water Resours. J. 28 (2), 153–172.
Li, Y.P., 2012. Study of Ecological Water Requirement of Tuhai River Watershed Based on SWAT Model. Ocean University of China, QingDao.
Li, X.F., Huang, D.M., Xie, W.X., et al., 2006. Current status of spawning grounds of fish with pelagic eggs in the middle reaches of Hanjiang River. J. Dalian Fish. College 21 (2), 105–111.
Li, Q., Bai, X., Lu, G., Zou, Z., 2011. Impact of the Three Gorges reservoir operation with different schemes on the downstream ecological water use. J. Hydroelectr. Eng. 30, 124–128.
Li, Q., Yu, M., Zhao, J., Cai, T., Lu, G., Xie, W., Bai, X., 2012. Impact of the Three Gorges reservoir operation on downstream ecological water requirements. Hydrol. Res. 43, 48–53.
Liu, C.M., Men, B.H., Song, J.X., 2007. River ecological water demand estimation of ecological hydraulic radius method. Prog. Nat. Sci. 17 (1), 42–48.
Liu, C.M., Zhao, C.S., Xia, J., Sun, C.L., Wang, R., Liu, T., 2011. An instream ecological flow method for data-scarce regulated rivers. J. Hydrol. 398, 17–25.
Mackie, J.K., Chester, E.T., Matthews, T.G., Robson, B.J., 2013. Macroinvertebrate response to environmental flows in headwater streams in western Victoria, Australia. Ecol. Eng. 53, 100–105.
Meyers, P.J., Belk, M.C., 2014. Shape variation in a benthic stream fish across flow regimes. Hydrobiologia 738 (1), 147–154.
Napiórkowska-Krzebietke, A., Dunalska, J., 2015. Phytoplankton-based recovery requirement for urban lakes in the implementation of the Water Framework Directive's ecological targets. Oceanolog. Hydrob. Stud. 44, 109–119.
Nelson, S.M., Lieberman, D.M., 2002. The influence of flow and other environmental factors on benthic invertebrates in the Sacramento River, USA. Hydrobiologia 489 (1), 117–129.
Neugirg, F., Stark, M., Kaiser, A., et al., 2016. Erosion processes in calanchi in the Upper Orcia Valley, Southern Tuscany, Italy based on multitemporal high-resolution terrestrial LiDAR and UAV surveys. Geomorphology 269, 8–22.
Pan, B., Wang, H., Ban, X., Yin, X., 2015. An exploratory analysis of ecological water requirements of macroinvertebrates in the Wuhan branch of the Yangtze River. Quat. Int. 380, 256–261.
Peng, T., Chen, X.H., Wang, G.X., Li, Y.H., 2012. Multi-objective evaluation model for minimum environmental flows based on wetted perimeter method. Adv. Sci. Technol. Water Res. 32, 6–10.
Pierzchala, M., Talbot, B., Astrup, R., 2014. Estimating soil displacement from timber extraction trails in steep terrain: application of an unmanned aircraft for 3D modelling. Forests 5 (6), 1212–1223.
Pool, T.K., Olden, J.D., 2015. Assessing long-term fish responses and short-term solutions to flow regulation in a dryland river basin. Ecol. Freshw. Fish 24 (1), 56–66.
Ruzgienė, B., Berteška, T., Gečyte, S., Jakubauskienė, E., Aksamitauskas, V.Č., 2015. The surface modelling based on uav photogrammetry and qualitative estimation. Measurement 73, 619–627.
Scharbert, A., Borcherding, J., 2013. Relationships of hydrology and life-history strategies on the spatio-temporal habitat utilisation of fish in European temperate river floodplains. Ecol. Ind. 29, 348–360.
Shang, L., Li, Z.L., Sun, W., Wang, Z.G., 2014. Estimation of river ecological base flow based on distributed hydrological model of HIMS. Res. Soil Water Conserv. 21, 100–103.
Shokoohi, A., Hong, Y., 2011. Using hydrologic and hydraulically derived geometric parameters of perennial rivers to determine minimum water requirements of ecological habitats (case study: Mazandaran Sea Basin-Iran). Hydrol. Process. 25, 3490–3498.
Stalnaker, C., Lamb, B.L., Henriksen, J., Bovee, K., Bartholow, J., 1995. The instream flow incremental methodology: a primer for IFIM. In: DTIC Document.
Tazioli, A., 2009. Evaluation of erosion in equipped basins: preliminary results of a comparison between the Gavrilovic model and direct measurements of sediment transport. Environ. Geol. 56 (5), 825–831.
Tazioli, A., Conversini, P., Peccerillo, A., 2012. Hydrogeological and geochemical characterisation of the Rock of Orvieto. Environ. Earth Sci. 66 (1), 55–65.
Tazioli, A., Mattioli, A., Nanni, T., Vivalda, P.M., 2015. Natural hazard analysis in the Aspio equipped basin. In: Engineering Geology for Society and Territory-Volume 3. Springer International Publishing, pp. 431–435.
Tharme, R.E., 2003. A global perspective on environmental flow assessment: emerging trends in the development and application of environmental flow methods for rivers. River Res. App. 19, 397–441.
Tikkanen, O., Heinonen, T., Kouki, J., Matero, J., 2007. Habitat suitability models of saproxylic red-listed boreal forest species in long-term matrix management: cost-effective measures for multi-species conservation. Biol. Conserv. 140 (3), 359–372.
Trippel, E.A., Chambers, R.C. 1997. Introduction: the early life history of fishes and its role in recruitment processes. FISH AND FISHERIES SERIES, 21: xxi-xxix.
Turner, D., Lucieer, A., Wallace, L., 2014. Direct georeferencing of ultrahigh-resolution UAV imagery. IEEE Trans. Geosci. Remote Sens. 52 (5), 2738–2745.
Vadas, R.L., Orth, D.J., 2001. Formulation of habitat suitability models for stream fish guilds: do the standard methods work? Trans. Am. Fish. Soc. 130, 217–235.

Vismara, R., Azzellino, A., Bosi, R., et al., 2001. Habitat suitability curves for brown trout (Salmo trutta fario L.) in the river Adda, northern Italy: comparing univariate and multivariate approaches. Regul. Rivers: Res. Manage. 17, 37–50.
Wakeley, J.S., 1988. A method to create simplified versions of existing habitat suitability index (HSIHSI) models. Environ. Manage. 12 (1), 79–83.
Wang, J.W., 1992. The reproductive biology of Gobiocypris rarus. Acta Hydrobiol. Sin. 2, 165–174.
Wang, Q.G., Li, J., Li, K.F., Li, R., 2009. Modification of wetted perimeter method for determining the ecological flow requirement. J. Hydraulic Eng. 40, 550–555.
Wang, J.N., Dong, Z.Y., Liao, W.G., 2013b. Based on hydrological method for evaluating the ecological environment of the response relationship between the water - in the three gorges reservoir and dam under river as an example. Sci. Sinica Technol., 715–726
Weaver, W., Shannon, C.E., 1949. The Mathematical Theory of Communication. University of Illinois, Urbana.
Wilbers, G., Becker, M., Sebesvari, Z., Renaud, F.G., 2014. Spatial and temporal variability of surface water pollution in the Mekong Delta, Vietnam. Sci. Total Environ. 485, 653–665.
Wu, W., Xu, Z., Yin, X., Zuo, D., 2014. Assessment of ecosystem health based on fish assemblages in the Wei River basin, China. Environ. Monit. Assess. 186, 3701–3716.
Xu, Z.X., Wang, H., Dong, Z.C., Tang, K.W., 2005. Theory and Practice of River and Lake Ecological Water Requirement. China WaterPower Press, BeiJing.
Yang, Y.C.E., Cai, X., Herricks, E.E., 2008. Identification of hydrologic indicators related to fish diversity and abundance. a data mining approach for fish community analysis. Water Resour. Res. 44.
Yang, H., Flower, R.J., Thompson, J.R., 2013. Sustaining China's water resources. Science 339, 141.
Yu, L.J., Chen, H.M., Wang, L., 2016. Study of ecological instream flow requirement of Jialu River based on improved wetted perimeter method. Adv. Sci. Technol. Water Resour. 36, 5–9.
Zarco-Tejada, P.J., Diaz-Varela, R., Angileri, V., Loudjani, P., 2014. Tree height quantification using very high resolution imagery acquired from an unmanned aerial vehicle (UAV) and automatic 3D photo-reconstruction methods. Eur. J. Agron. 55, 89–99.
Zhang, W., Zhang, X.L., Li, L., et al., 2007. Urban forest in Jinan City: distribution, classification and ecological significance. Catena 69 (1), 44–50.
Zhang, Z.G., Shao, Y.S., Xu, Z.X., 2010. Prediction of urban water demand on the basis of Engel's coefficient and Hoffmann index: case studies in Beijing and Jinan, China. Water Sci. Technol. 62 (2), 410–418.
Zhao, C.S., Liu, C.M., Xia, J., 2008. Instream ecological flow of dammed river-a case study of huaihe river. J. Nat. Resour. 23 (3), 400–411.
Zhao, C.S., Yang, S.T., Liu, C.M., et al., ao et al., 2015 b. Linking hydrologic, physical and chemical habitat environments for the potential assessment of fish community rehabilitation in a developing city. J. Hydrol. 523, 384–397.
Zhao, C.S., Yang, S.T., Xiang, H., Liu, C.M., Zhang, H.T., et al., 2015a. Hydrologic and water-quality rehabilitation of environments for suitable fish habitat. J. Hydrol. 530, 799–814.
Zohmann, M., Pennerstorfer, J., et al., 2013. Modelling habitat suitability for alpine rock ptarmigan (Lagopus muta helvetica) combining object-based classification of IKONOS imagery and Habitat Suitability Index modelling. Ecol. Model. 254, 22–32.